Seismic Evaluation of Pile Foundation Systems Subjected to Rocking

Pedro F. Silva, & Majid T. Manzari
The George Washington University, Washington, DC, U.S.A.

SUMMARY:
This research investigates the rocking of pile caps over their piles. Rocking of pile caps is investigated numerically by considering the piles are not vertically anchored to the pile cap by the traditional anchorage reinforcement. A suitable detail for the connection of pile heads to the pile caps is proposed in which transverse displacements of the pile heads relative to the pile cap are restrained, but the pile cap is allowed to uplift from the piles. Using this detail, a seismic evaluation of pile caps with and without rocking was undertaken and results are outlined in this paper. Besides the benefit that no bending moments develop at the piles heads, it is shown that the factor of safety against overturning and lateral deformations of the pile cap are not compromised and in some cases there is a reduction of 20% in the design shear force and drift demands on the columns.

Keywords: Seismic Evaluation, Rocking, Pile Foundation Systems

1. INTRODUCTION

Damage inspections following previous earthquakes have shown that a large number of structures had escaped serious damage as a result of their ability to rock on their footing pads. Previous research has also confirmed the suitability of using rocking of shallow foundations as a means of base isolation and thus reducing damage to structures during earthquakes. Although previous research has clearly shown the benefits of using rocking, this philosophy is a major departure from current design codes which do not allow rocking in design. In fact design codes in the US explicitly state that "*Foundation rocking shall not be used for the design of bridges*".

Foundation rocking combined with the inelastic properties of soil may be beneficial in a strong seismic event for several reasons. First, uplift reduces the contact area between the soil and the foundation and introduces radiation damping in the system. Second, rocking provides a means for self-centering, leading to structures that are more resistant to P-Delta effects. However, design codes have not moved towards accepting foundation rocking because permanent settlements combined with rotations of the foundation are likely to be present after rocking. Combined with the fact that nonlinearities below ground level are not allowed, foundation rocking is not permitted in the design of bridges in the US.

The research outlined in this paper presents an extension to foundation rocking of spread footings by considering rocking of pile caps on cast-in-place-steel-shell (CISS) piles. In this research, rocking of pile caps is investigated by providing a detail such that CISS piles are not rigidly attached to the pile cap by the traditional anchorage reinforcement. In California, CISS piles account for over 1/3 of the piles driven by Caltrans. These CISS piles are also common in other states such as Oregon, Washington, and Alaska. Other advantages in using driven CISS piles that are subsequently filled with cast-in-place reinforced or unreinforced concrete, especially in seismic regions, is the satisfactory performance of steel casings to enhance the ductility capacity of reinforced concrete sections through confinement of the concrete core (Chai et al., 1991; Priestley et al., 1996; Silva and Seible, 2001). The

main problem of this connection detail is that when the CISS pile rotates the contact forces between the CISS pile and the concrete causes a wedging effect that induce early and undesirable damage to the pile cap. Many tests are reported in the literature documenting extensive damage at the connection to the pile cap (see Figure 1a, Silva and Seible, 2001). This research can lead to a resolution of this damage condition by avoiding the anchorage reinforcement into the pile cap and thus the prying action effect of the steel shell on the pile cap. This concept is discussed next.

Rocking of pile caps is investigated numerically by considering the CISS piles are not vertically anchored to the pile cap by the anchorage reinforcement depicted in Figure 1b. Instead the pile cap is allowed to uplift from the piles. To achieve this response, an engineered material is placed in-between a steel sleeve that is embedded into the pile cap and set inside the CISS piles. This steel sleeve will not provide tension capacity to the connection but only provide transfer of shear and compression forces. An added benefit of this connection is that the steel shell is terminated below the pile cap, thus, avoiding the prying action and subsequent damage to the underside of the pile cap. A numerical model is outlined in this paper that can mimic the response of the connection under seismic effects. Using the numerical model of the detailed connection, an extensive seismic evaluation of pile caps with and without rocking about their underlining piles was undertaken and results of this seismic evaluation is outlined in this paper.

Seismic evaluation of pile caps have shown an improved response when the pile caps are allowed to rock by: reducing the design shear force in the columns by as much as 20 to 30%, a decrease in ductility demand in the columns, and no bending moments developed at the head of the piles. However, it is important to emphasize that in each transverse direction the pile cap is restrained by the piles. Besides the benefit that no moments develop at the head of the piles, results further show that the factor of safety against overturning and deformations of the pile cap are not compromised. These results are further corroborated in this paper.

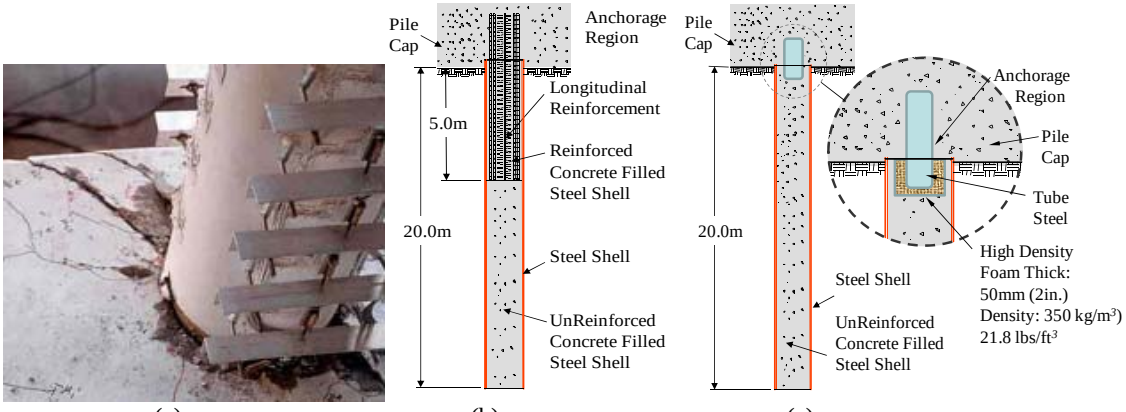

(a) Damage to CISS Pile under Laboratory Conditions (Silva and Seible, 2006)
(b) Current CISS Detail Connection to Pile Cap
(c) Proposed CISS Pipe Pile Detail Connection to Pile Cap to Achieve Rocking of Pile Foundation Systems

Figure 1. Current and Proposed Steel-Shell Pipe Pile (Steel-Shell) Detail Connection to Pile Cap

2. ROCKING OF SHALLOW FOUNDATIONS

Rocking of a rigid body subjected to lateral base ground motions was first addressed by G.W. Housner in 1963 (Housner 1963). Inspections immediately after the Chilean earthquake of 1960 had shown that a large number of slender structures survived this earthquake, while other structures, apparently more stable, toppled over their footing pads. Housner was motivated by these events and concluded that the ability of structures to survive the earthquake was mainly a result of their ability to rock on their footing pads. Since then, many researchers have proposed using rocking of shallow foundations as a means of base isolation and thus reducing damage to structures during earthquakes. In his 1963 paper,

Housner developed the closed form solutions for the inverted pendulum Housner established by implementing the following assumptions: (1) the rocking body and its base are considered to be rigid, (2) sliding and uplift were neglected, and (3) the loss of energy from the rocking impacts is described by the factor of energy reduction. The second assumption (i.e. sliding and uplift are neglected) fails to duplicate the point of the base of the rigid block when it loses contact with the ground. This is an important consideration and other researchers have considered the uplift effects on the rocking response of rigid bodies.

Ishiyama (1982) and Lipscombe and Pellegrino (1991) have studied the importance of considering the instance when the response of the body can be completely detached from the base, thus violating Housner's second assumption. Psycharis and Jennings (1983) proposed an improved model which considered the flexibility of the ground. This model provided concentrated springs and dampers at the corners of the rigid body similar to the Winkler type of foundation modelling. Most recently, Sivapalan and Kutter (2008) investigated the capacity, settlement, and energy dissipation of shallow footings subjected to rocking and concluded that rocking leads to an improvement in performance of structures during seismic loading. Some of the improvements that have been reported are: (1) rocking does not lead to large permanent settlements, (2) has a self-centering characteristic associated with uplift and gap closure, and (3) dissipates seismic energy that translates in 20% damping ratio. The analytical model developed in this paper will address and investigate these issues by considering "compression plus shear-only" contact elements at the connection of the pile cap to the piles.

3. ANALYTICAL MODELS

Rocking of pile caps was investigated by considering that the piles are not vertically anchored to the pile cap by the traditional anchorage reinforcement. Instead the pile cap is allowed to undergo vertical displacements relative to the piles heads. To achieve this response, an engineered material is placed in-between a steel sleeve that is embedded into the pile cap and set inside the CISS piles. This steel sleeve will not provide tension capacity to the connection but only provide transfer of shear and compression forces. In total 972 simulations were performed, out of which 486 simulations were performed for pile groups not considering rocking, and the remaining 486 simulations were performed for pile groups considering rocking.

3.1. Prototype Structure and Analysis Matrix

A 3-D 4×4 pile group was designed and subsequently evaluated via a nonlinear finite element analysis under a set of three distinctive earthquake records. The finite element model used in this seismic evaluation was modelled based on the prototype structure presented in Figure 2 and evaluated under the analysis matrix presented in Table 1.

Table 1. Matrix for Seismic Evaluation of Pile Foundation Systems Subjected to Rocking

Earthquake Record	Column Aspect Ratio, α_C	Axial Load Ratio, β	Pile Spacing Ratio, α_P	Soil Type	Earthquake Direction
Synthetic Record	3	6	2.0	Soft	Uni-Directional
Northridge, CA, 1994	4	9	2.5	Medium	Bi-Directional
Inca, Peru, 2007	5	12	3.0	Stiff	--

The finite element analyses were conducted using Opensees program (Mazzoni et al., 2006). As depicted in Table 1, the simulations reflected variations in the modelling parameters by considering: (1) three earthquakes, (2) three column aspect ratios, (3) three axial load levels, (4) three piles spacing, (5) three soil types, and (6) uni-directional and bi-directional of loading were considered in the analysis. The earthquake records considered for this study are depicted in Figure 3. Comparing the last significant earthquake in CA (Northridge, 1994, M6.7) to the latest earthquake in Ica, Peru (2007, M8.0), it is clear from Figure 3a and 3b that the PGA acceleration at the chosen stations is nearly the

same (see Figure 3b). A major difference between these two records is that while in the Northridge earthquake the spectral displacement (SD) (see Figure 3c) continuously increases up to its maximum value, for the Peruvian record the SD has a sharp rise shortly after the 2-second period. A synthetic earthquake record was also created to simulate as close as possible the Northridge and Ica Peru records with the objective of creating a smoother spectral acceleration and displacement response spectrum.

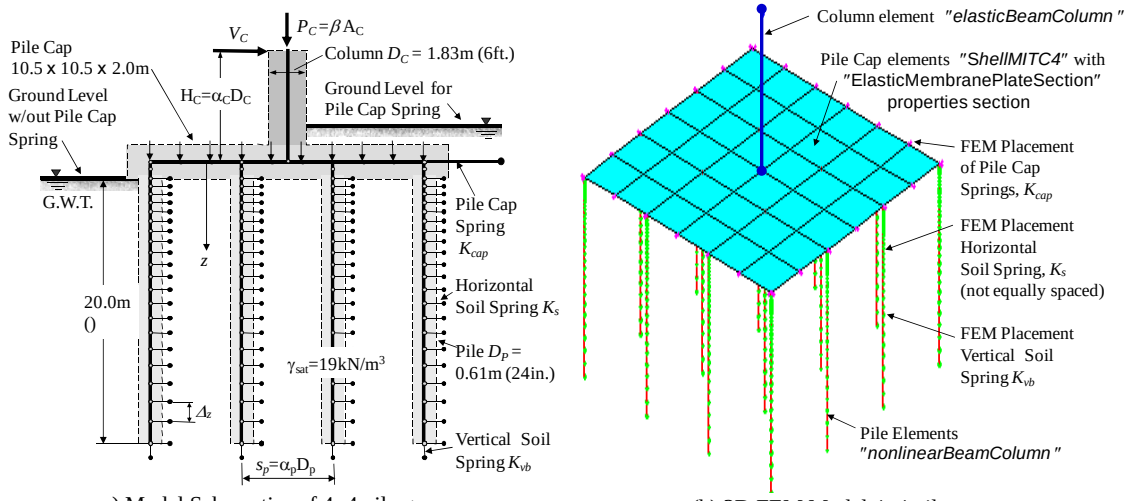

a) Model Schematics of 4×4 pile group (b) 3D FEM Model 4×4 pile group

Figure 2. Prototype Structure and 3D FEM Model for Time History Analysis

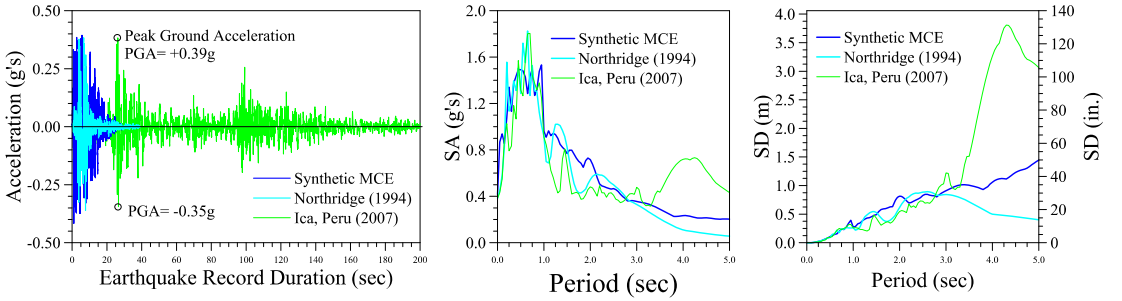

(a) Earthquake Records (b) Spectral Acceleration, SA (c) Spectral Displacement, SD

Figure 3. Earthquake Records used in this study

3.4. Column Modelling Considerations

The seismic design demands on the system were obtained by modelling the columns with linear elastic elements and using the cracked stiffness properties given by the initial bilinear slope of the columns capacity presented in Figure 4a. OpenSees supports multiple types of elements. The *elasticbeamcolumn* element with linear elastic behaviour was used for modelling of the columns. This would allow for to obtain the elastic shear design force for the columns and provide for a more direct form of comparison between the 2 sets of simulations. In addition to the self-weight of each member, the weight of the pile cap and axial loads imposed on the column were also considered in the analyses. The axial loads on the columns were 6%, 9% and 12% corresponding to approximately 286, 430, and 580 kN (1270, 1910, and 2540 kips), respectively.

3.5. Pile Modelling Considerations

The piles were the standard Caltrans Class 200 pile, which consisted of a steel shell with embedment length of 127mm (5in.) into the pile cap. The piles were arranged in a 3D 4×4 pile group. The pile cap was modelled as linear elastic with the stiffness computed based on a section with the dimensions of

10.7×10.7×2.44m (35×35×8ft). The piles were modelled with *nonlinearBeamColumn* elements and only 2 integration points were considered in the model to reduce the computational running time. The pile cross section was modelled by using a *fiber section*, which has the capabilities of modelling a geometric configuration by subdividing the section into *patches* or sub-regions. The sub-regions and the equivalent uniaxial material properties are depicted in Figure 4b. For each fiber section, material properties representing the stress-strain relationships for the concrete and the reinforcing steel were assigned by developing *uniaxialMaterial* objects. As shown in Figure 4b, thematerial model *Concrete07* was used to simulate both the confined and unconfined regions. The internal reinforcement was modelled according to the *Reinforcingsteel* material option. This material model provides control over the transition from the elastic to the plastic region and was used to construct the *uniaxial* steel material properties. The *Steel02* material option was used to model the steel shell and was only provided beyond the bond length of the steel shell; however, its confining action was considered for the entire length of the piles. To develop the tensile stresses present in the steel shell an average bond strength of 2.0MPa (290 psi) was assumed for the analysis, leading to a development length of approximately 1.5m (~5 ft) for the steel shell (Silva and Manzari, 2008).

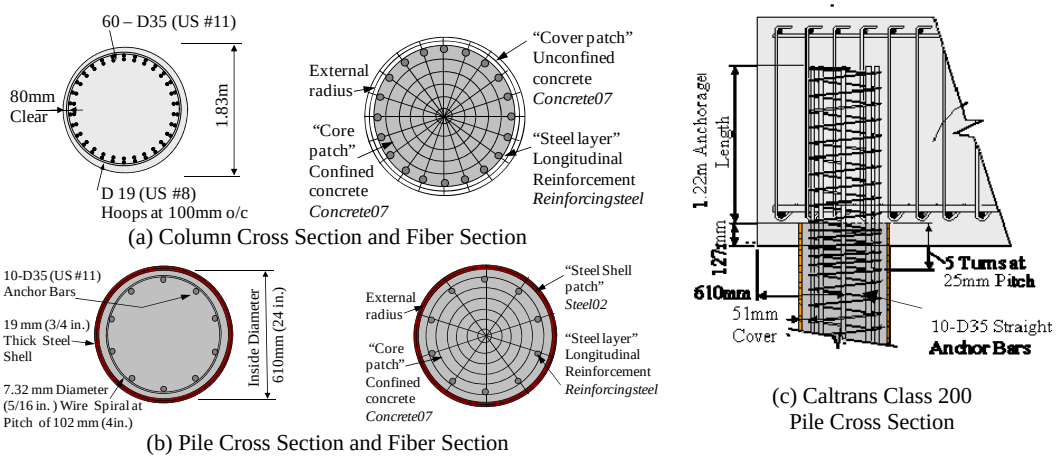

(a) Column Cross Section and Fiber Section

(b) Pile Cross Section and Fiber Section

(c) Caltrans Class 200 Pile Cross Section

Figure 4. Modelling of Prototype Column and Pile Cross Sections

3.6. Soil Modelling

Modelling of the soil effects around the piles was established with discrete nonlinear spring elements in terms of the Winkler foundation method. In Opensees this can be established using *zeroLength* elements with the distribution of nodes and elements depicted in Figure 5a. As shown, six beam elements with a length of $D_p/6$ were used at the pile head, and using a quadratic regression, the element sizes were increased to $D_p/2$ at the pile tip. Figure 5b depicts one vertical *zeroLength* elements (*t-z* spring), and four horizontal compression-only *zeroLength* elements (*p-y* spring) were placed around the four sides of the piles. In addition, only one vertical *zeroLength* element (*q-w* spring) was placed at the tip of the piles. Formulation of the soil properties were representative of cohesive soft, medium and stiff clay soils. Further, modelling considerations are discussed next.

3.6.1. Soil Properties: p-y Springs Positioned along the Height of the Piles

A bilinear relation was implemented as a simplified form of *p-y* curves. Change of the soil properties during cyclic response may lead to permanent deformations in the soil layer, and the soil ultimate strength and stiffness decay with each cycle. To accomplish this idealized soil response, *zerolength* elements were placed on all four sides of the piles and three material objects were assembled in series to achieve the desired response, which consisted of compression-only behaviour, gapping and cyclic degradation. These properties were implemented in Opensees by using: (1) the *uniaxialMaterial ENT* object to model the compression-only behaviour, (2) the *uniaxialMaterial ElasticPPGap* object to model the gapping behaviour interface between the pile and the soil, and (3) the *uniaxialMaterial Hysteretic* object to capture the hysteretic cyclic load-deformation degradation of the soil. This model

is schematically shown in Figure 6a where the spring stiffness at any depth, K_{py}, and soil ultimate pressure, p_{ult}, were obtained per Eqs. (3.1) and (3.2).

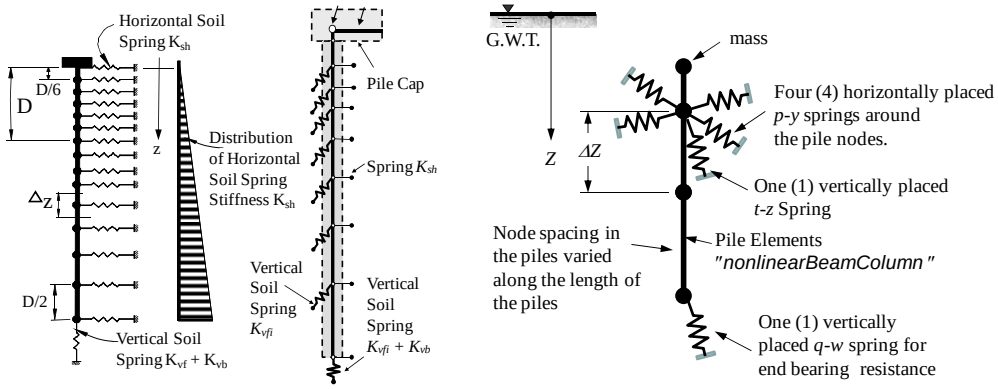

(a) Soil Springs Distribution Around Piles (b) Soil Modeling at Single Node

Figure 5. Soil Modelling Around the Piles

$$K_{py} = k_h \, \Delta_z Z \left(\frac{D_p}{D^*} \right) \leq p_{ult} \, Z \left(\frac{D_p}{D^*} \right) \tag{3.1}$$

$$p_{ult} = 5 \, K_p \, \sigma'_v \qquad \text{with} \qquad K_p = \frac{1 + sin\varphi_s}{1 - sin\varphi_s} \tag{3.2}$$

Where k_h is the coefficient of horizontal subgrade reaction modulus, Δ_Z is the spacing between the springs at a depth Z, K_p is the passive earth pressure coefficient, φ_s is the soil friction angle, and σ'_v is the vertical effective stress at a depth Z.

3.6.2. Soil Properties: p-y Springs Positioned in front of the Pile Cap

The seismic response of the pile group was also characterized in terms of the passive pressures that mobilize in front of the pile cap. This was conducted by placing *zerolength* elements in front of the pile cap according to the model illustrated in Figure 2a and Figure 6a. The pile cap spring stiffness, K_{cap}, was computed according to the expression (Silva and Manzari, 2008):

$$K_{cap} = k_h \frac{H_{cap}^2}{2} \left(\frac{W_{cap}}{D^*} \right) \tag{3.3}$$

Where H_{cap} and *Wcap* are the height and width of the pile cap, respectively, and the ultimate soil pressure was obtained per Eq. (3.2).

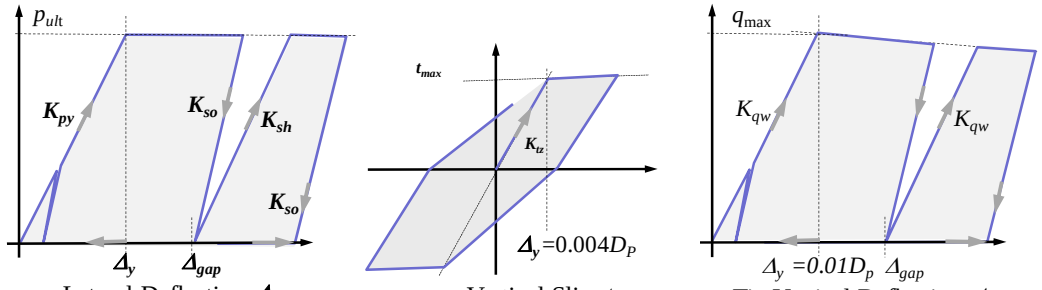

(a) *p-y Springs* Hysteretic (b) *t-z Springs* Hysteretic (c) *q-w Springs* Hysteretic

Figure 6. Soil Hysteretic Models

3.6.3. Soil Properties: t-z Skin Friction Resistance Pile-Soil Model

The soil-pile skin friction resistance was modeled by placing vertically oriented *zerolength* elements along the length of the piles. Starting at the head of the piles the skin-friction resistance stiffness was described in terms of Eq. (3.4) using the *t-z* relationships developed by Aschenbrener and Olson (1984). The cyclic response of these *t-z* springs is illustrated in Figure 6b. The *t-z* relationship flattens as the shear stress reaches t_{max} and the initial stiffness, K_{tz}, is assumed linear up to a relative displacement of 0.4% (Silva and Manzari, 2008).

$$K_{tz} = k_{tf}\left(\pi D_p\right)\Delta Z \tag{3.4}$$

3.6.4. Soil Properties: q-w End Berating Resistance

The soil end bearing resistance stiffness, K_{qw}, was calculated by using the *q-w* relationship proposed by Aschenbrener and Olson (1984) for piles embedded in clays. The *q-w* relationship was assumed bilinear, and the initial slope of the *q-w* curve was obtained by:

$$K_{qw} = K_q A_p\left(\frac{D_p}{D^*}\right) \tag{3.5}$$

$$K_q = \frac{9 s_u}{0.01 D_p} \tag{3.6}$$

Where A_p and D_p are the area and the diameter of the pile, s_u is the average unconfined compression strength of the soil from $3D_{tip}$ below to $3D_{tip}$ above the pile tip. Once the tip displacement reaches 1% of the pile diameter the soil pressure at the pile tip reaches its maximum value, q_{max}, and remains constant with a limit given by Eq. (3.7) (Aschenbrener and Olson, 1984). In Eq. (3.7) N_c ranges from 0.0 to 20.0 and is independent of the soil shear strength, and, in this work, N_c was set to 9.

$$q_{\max} = N_c . s_u \tag{3.7}$$

4. SEISMIC EVALUATION RESULTS

In the next sections the finite element simulation results will be evaluated based on: (1) the design shear force demand on the columns, (2) the system drift demand on the columns, and (3) the factor of safety against system overturning. To further simplify discussion of the results, these simulations were grouped in 9 sets corresponding to the runs with different column aspect and axial load ratios. These are clearly defined in Table 2. For instance, set [1] corresponds to the simulations containing all the results for columns with an aspect ratio of $3D_C$ and an axial load ratio of $6\%A_C$.

4.1. Column Shear Force Design Demand

Figure 7a presents the results corresponding to the column shear force design demand for relations accounting for [Rocking], as shown in the y-axis, and [No Rocking], as shown in the x-axis. As a clarification this same graphical presentation of the simulation results will be implemented in the discussion of the other significant results. It is clear from Figure 7a that the main diagonal line (i.e. solid lines) indicates the design demand for rocking and no rocking are nearly the same. Simulation results that follow below the line designated as "*Reduction>20%*" indicate that rocking will reduced the shear force design demand for the columns by as much as 20%. Conversely, those results situated above the line designated as "*Increase>20%*" indicate that rocking will increase the shear force design demand for the columns in excess of 20%. Those results within the boundary of these two lines indicate there is no appreciable difference in the column shear force design demand if rocking is considered in the analysis or not. From this figure one may observe that for a significant number of runs the column shear force design demand was reduced when rocking was considered in the analysis, and only in a few of the runs rocking did not contribute to a reduction in shear force demand.

Table 2. Set Number Analysis Parameters

Set	Column Height Aspect Ratio	Column Axial Load Ratio
[1]	$H_C = 3\ D_C$	$P_C = 6\%\ A_C$
[2]	$H_C = 3\ D_C$	$P_C = 9\%\ A_C$
[3]	$H_C = 3\ D_C$	$P_C = 12\%\ A_C$
[4]	$H_C = 4\ D_C$	$P_C = 6\%\ A_C$
[5]	$H_C = 4\ D_C$	$P_C = 9\%\ A_C$
[6]	$H_C = 4\ D_C$	$P_C = 12\%\ A_C$
[7]	$H_C = 5\ D_C$	$P_C = 6\%\ A_C$
[8]	$H_C = 5\ D_C$	$P_C = 9\%\ A_C$
[9]	$H_C = 5\ D_C$	$P_C = 12\%\ A_C$

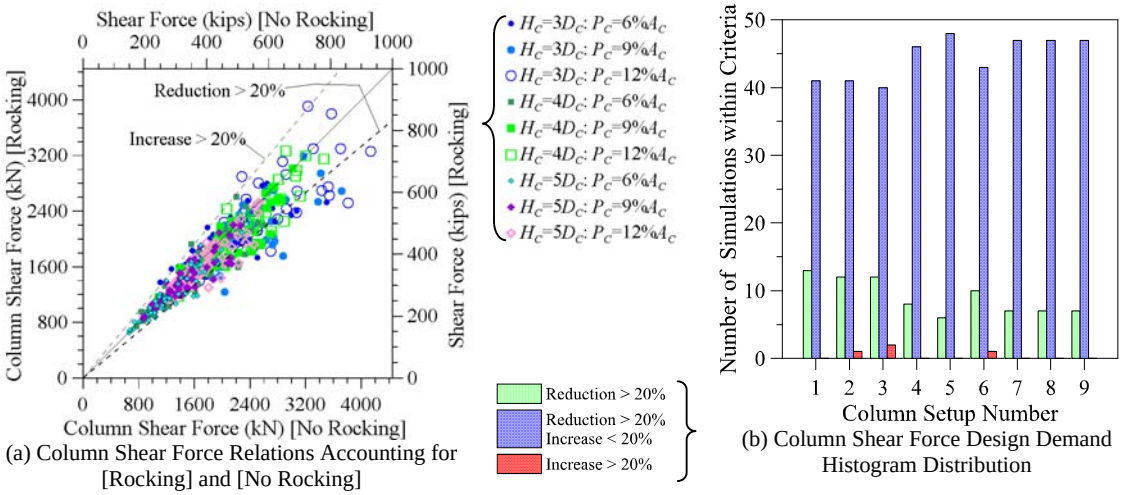

(a) Column Shear Force Relations Accounting for [Rocking] and [No Rocking]

(b) Column Shear Force Design Demand Histogram Distribution

Figure 7. Column Shear Force Design Demand

More precisely, in 24% of the simulations the shear force design demand was reduced by more than 20% when rocking was considered, and in less than 3% of the simulations did the shear force design demand increased by more than 20% when rocking was considered. In the remaining 75% of the runs rocking did not significantly affect the shear force design demand in. A visual impression of the distribution of these data is graphically depicted in the histogram of Figure 7b. This figure shows the distribution of the data according to the set numbers outlined in Table 2. One important observation from this histogram is that in only a very few number of runs did rocking increase the design shear force demand on the columns. These columns are depicted by the solid (or red shading area). However, it is important to note that there are many other benefits when considering rocking. These may include reducing or even avoiding altogether the extensive damage at the connection to the pile cap (see Figure 1a), and as importantly reduction in construction time and fabrication by avoiding the need for the anchorage reinforcement as shown in Figure 1b.

4.2. System Drift Ratio Demand

System drift ratio demand is another design variable that was used in this paper to evaluate the impact that rocking can have on the seismic response of pile groups. Figure 8 presents the results corresponding to the drift demands for systems with [Rocking] and [No Rocking]. As before, results along the main diagonal line indicate that the drift demand for rocking and no rocking are nearly the same. Runs below the line designated as "*Reduction>20%*" indicate that there was a reduction in the design drift demand by as much as 20%. Conversely, those results above the line designated as "*Increase>20%*" depict an increase in the design drift demand by as much as 20% when rocking was considered in the analysis. More precisely, in less than 2% of the simulations the system drift design demand was reduced by more than 20% when rocking was considered, and in less than 5% of the simulations did the system drift design demand increased by more than 20% when rocking was

considered. In the remaining 97% of the runs rocking did not significantly affect the system drift design demand. As previously stated lateral deformations of the system are not compromised when considering rocking of the pile group system.

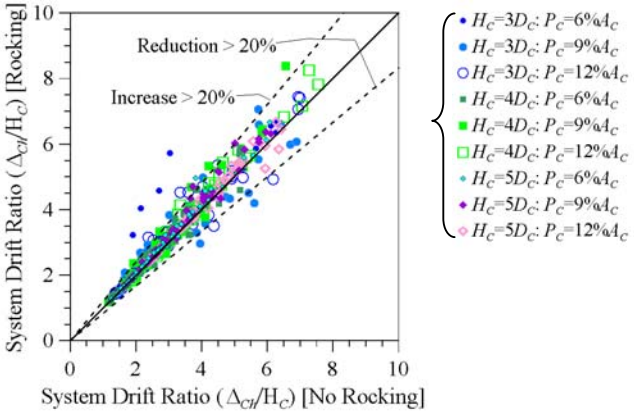

Figure 8. System Drift Ratio Accounting for [Rocking] and [No Rocking]

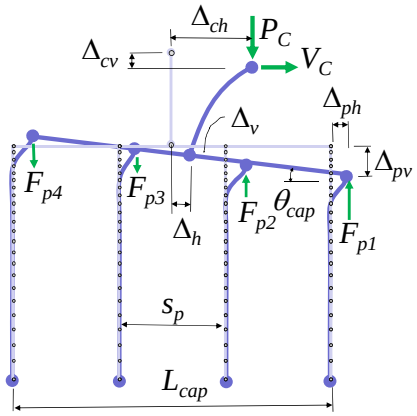

Figure 9. Factor of Safety against Overturning

4.3. Factor of Safety against Overturning

The factor of safety against overturning was established based on the graphical depiction outlined in Figure 9 and is computed using Eqs. (4.1) thru (4.3). Based on these relations the factor of safety against overturning for simulations considering [Rocking] and [No Rocking] are presented in Figure 9.

$$OTM = V_C \times \left(H_C + \Delta_{cv} - \Delta_h\right) + P_C \times \left(\Delta_{ch} - \Delta_h\right) \tag{4.1}$$

$$RM = \sum_{i=1}^{5} F_{pi}\left(L_i - \frac{L_{cap}}{2}\right)cos(\theta) \tag{4.2}$$

$$FS = \frac{RM}{OTM} \tag{4.3}$$

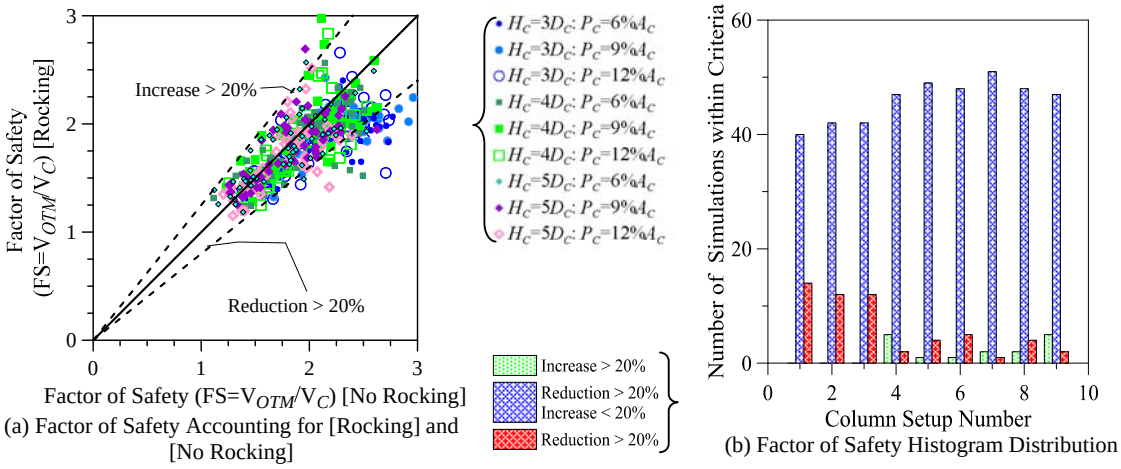

(a) Factor of Safety Accounting for [Rocking] and [No Rocking]

(b) Factor of Safety Histogram Distribution

Blank line 10 pt

Figure 10. Factor of Safety against Overturning

Where *OTM* is the overturning moment at the base of the column due to V_C and P_C, *RM* is the resisting moment, F_{pi} are the forces in the piles, L_i is the distance from the pile '*i*' to the right side of the pile cap, L_{cap} is the length of the pile cap, *FS* is the factor of safety, and the other variables are depicted in Figure 9. Figure 10a presents the results corresponding to the factor of safety against overturning

results accounting for [Rocking], and [No Rocking]. Results along the main diagonal line clearly suggest that considering rocking of pile foundation systems, per the proposed detail shown in Figure 1b, the factor of safety against overturning was not compromised and in a few cases the factor of safety was actually increased beyond 20%. Runs that follow below the line designated as "*Reduction>20%*" indicate that rocking will reduce the factor of safety against overturning by as much as 20%. Those results above the line designated as "*Increase>20%*" indicate that rocking will increase the factor of safety against overturning in excess of 20%. Those results within the boundary of these two lines indicate there is no appreciable difference if rocking is considered in the analysis or not. The histogram of Figure 10b clearly show that a significant number of simulations showed an increase in the factor of safety. More precisely, in 24% of the simulations the factor of safety was increased and less than 2% of the runs showed that rocking reduced the factor of safety.

CONCLUSIONS

Previous research has clearly shown the suitability of using rocking of shallow foundations and mobilizing the inelastic properties of the soil beneath a shallow foundation as a possible mechanism and/or location for the inelastic behavior of the system to occur during major earthquakes. The research outlined in this paper presents a departure from rocking of shallow foundations by extending rocking to be considered for entire pile group system. In this research, rocking of pile caps is investigated by providing an innovative detail that does not transfer tensile forces and bending moment to the underlying piles. The piles in this research consisted of CISS piles.

In many of the simulation runs there was an improved seismic response when the pile caps were allowed to rock over the underlying piles by: (1) reducing the design shear force demand in the columns, (2) a decrease in the design drift demand in the columns, and (3) an increased factor of safety against overturning. Certainly other benefits exists that go beyond seismic response and may include reducing or even avoiding altogether the extensive damage at the connection to the pile cap, and as importantly reduction in construction time and fabrication by avoiding the need for the anchorage reinforcement from the piles into the pile cap.

REFERENCES

Aschenbrenner, T. B., and Olson, R. E. (1984) "Prediction of settlement of single piles in clay." *Analysis and design of pile foundations*. American Society of Civil Engineers, Editor J. R. Meyer. 41-58.

Chai, H.Y., Priestley, M.J.N., Seible, F. (1991) "Seismic Retrofit of Circular Bridge Columns for Enhanced Flexural Performance," *ACI Journal Journal*, **88:5**, 572-584.

Housner, G.W. (1963) "The Behavior of Inverted Pendulum Structures During Earthquakes," *Bulletin of the Seismological Society of America*, **53:2**, 403-417.

Ishiyama, Y. (1982) "Motion of Rigid Bodies and Criteria for Overturning." *Earthquake Engineering And Structural Dynamics*, **10:5**, 635-650.

Lipscombe, R. P. and Pellegrino, S. (1991) " Free Rocking of Prismatic Blocks," *Journal of Engineering Mechanics*, **119:7**, 1387-1410.

Mazzoni, S., McKenna, F., Scott, M.H., Fenves, G.l. et al. (2006), "Open System for Earthquake Engineering Simulation User Command-Language Manual," OpenSees version 1.7.3, *Pacific Earthquake Engineering Research Center* (PEER), University of California, Berkeley.

Priestley, M. J. N., Seible, F., Calvi, M. (1996) *Seismic Design and Retrofit of Bridges*, John Wiley & Sons, Inc., New York, 672.

Psycharis, I.N. and Jennings, P.C. (1983) "Rocking of Slender Rigid Bodies Allowed to Uplift," *Earthquake Engineering and Structural Dynamics*, **11:1**, 57-76.

Silva, P. F., Seible, F. (2001) "Seismic Performance Evaluation of CISS Piles," *ACI Structural Journal*, **98:1**, 36-49.

Silva, P.F., and Manzari, M.T. (2008) "Nonlinear Pushover Analysis of Bridge Columns Supported on Full-Moment Connection CISS Piles on Clays," *EERI Earthquake Spectra*, **24: 3**, 751-774.

Sivapalan, G. and Kutter, B.L. (2008) "Capacity, Settlement, and Energy Dissipation of Shallow Footings Subjected to Rocking," *Journal of Geotechnical and Geoenvironmental Engineering*, **134:8**, 1129–1141.